Theoretical simulation of a polarization splitter based on dual-core soft glass PCF with micron-scale gold wire*

Qiang Liu(刘强), Shuguang Li(李曙光)†, Xinyu Wang(王新宇), and Min Shi(石敏)

Key Laboratory of Metastable Materials Science and Technology, College of Science, Yanshan University, Qinhuangdao 066004, *China*

(Received 15 May 2016; revised manuscript received 29 July 2016; published online 25 October 2016)

A polarization splitter based on dual-core soft glass photonic crystal fiber (PCF) filled with micron-scale gold wire is proposed. The characteristics of the polarization splitter are studied by changing the structural parameters of the PCF and the diameter of the gold wire with the finite element method (FEM). The simulation results reveal that the coupling length ratio of the soft glass-based PCF is close to 2 and the corresponding curve is more flat than that of the silica-based PCF. The broadband bandwidth is 226 nm in which the extinction ratio is lower than −20 dB by the soft glass-based PCF, i.e., from 1465 nm to 1691 nm which is competitive in the reported polarization splitters, and the bandwidth is just 32 nm by the silica-based PCF. The insertion loss by our polarization splitter is just 0.00248 dB and 0.43 dB at the wavelength of 1.47 μm and 1.55 μm. The birefringence is obviously increased and the coupling length is decreased by filling gold wire into the soft glass-based or the silica-based PCF. Also the birefringence based on the silica-based PCF is much larger than that based on the soft glass-based PCF whether or not the gold wire is introduced. The fabrication tolerance of the polarization splitter is also considered by changing the structural parameters. The polarization splitter possesses broad bandwidth, low insertion loss, simple structure and high fabrication tolerance.

Keywords: photonic crystal fiber, polarization splitter, extinction ratio

PACS: 42.81.–i, 42.81.Gs, 71.45.Gm **DOI:** 10.1088/1674-1056/25/12/124210

1. Introduction

To fulfill the ever-increasing transmission demands of optical communication systems, polarization division multiplexing (PDM) plays a pivotal role in manipulating optical signals. Polarization splitters, which are essential components for PDM and play a key role in optical fiber communication and sensing system, could split one beam into two orthogonal polarization lights. A polarization splitter based on mode coupling is a hot topic. The devices based on the mode coupling possess the advantage of short fiber length, but also possess the disadvantages of narrow bandwidths and low fabrication tolerances.[1–6] For example, a conventional fiber polarization splitter just can realize polarization splitting at the wavelength of 633 nm.[6] We have to design a broadband polarization splitter to adapt to the development of high-speed and broadband communication system.

In recent years, photonic crystal fibers (PCFs),[7] in which the air holes are periodically arranged and are parallel to the propagation direction, have attracted a great deal of interest. The special fibers are divided into two kinds. One is called index-guided PCF. The refractive index of the fiber core is higher than that of the cladding region, so the light could be bound in the fiber core by total internal reflection. The other one is photonic-bandgap PCF. The refractive index of the fiber core is lower than that of the cladding region, so then the light could be bound in the fiber core by photonic bandgap effect. All kinds of new products of PCF come into being as the development of manufacturing technology of PCF, which are not only applied to the conventional optical communication technology, but also widely used in the field of optical devices, such as fiber laser,[8] fiber amplifier,[9] supercontinuum,[10] dispersion compensation,[11] polarization rotator,[12] biosensors,[13] and other fields.

PCFs offer a great opportunity to develop broadband polarization splitters because of their remarkable tunability and unique optical properties. Zhang[14] obtained a polarization splitter by PCF in which the two cores are nonidentical, and a bandwidth of 80 nm is realized. The two high birefringence cores are vertically distributed, two polarization lights realize selective coupling, the X-polarization light couples between the two cores completely, and just a little energy of the Y-polarization light happens to couple. Kaitoh[15] designed a polarization splitter by a three-core PCF, in which the bandwidth is 37 nm. The phenomenon of resonant tunneling is used by the polarization splitter. The two cores of the PCF are identical, a high birefringence core separates them, and just one polarization light couples between the two cores. Chiang[16] proved a polarization splitter by a dual-core PCF, the bandwidth in which the extinction ratio is better than 13 dB is 30 nm, the polarization splitter possesses the advantage of a short length of 300 μm. Chen[17] proposed a polarization splitter which has a bandwidth of 101 nm, the two cores of the square-lattice PCF are asymmetric which results that just

*Project supported by the National Natural Science Foundation of China (Grant Nos. 61178026, 61475134, and 61505175).

†Corresponding author. E-mail: shuguangli@ysu.edu.cn

© 2016 Chinese Physical Society and IOP Publishing Ltd

one polarization light couples between the two cores completely and the other polarization light couples incompletely. Zhang[18] obtained a dual-core PCF polarization splitter which has high birefringence, and its bandwidth in which the extinction ratio is lower than −11 dB is 40 nm. Liu[19] designed a polarization splitter with a bandwidth of 20 nm, tellurite glass-based and three-core PCF has a better extinction ratio and coupling loss compared with silica-based PCF. Zhang[20] proposed a twin-core PCF and demonstrated that the silica bridges between the two cores are very important for the energy coupling through the air holes. Jiang[21] proved a PCF broadband polarization splitter, and its bandwidth is 249 nm, but two cores is so close that it is hard to separate two orthogonal polarization light beams. Liquid, liquid crystal, metal material, etc. could be injected into the cladding air holes to improved the coupling characteristics of PCF. Hameed[22] designed a liquid-crystal-core PCF, the bandwidth in which the extinction ratio is lower than −20 dB is 250 nm. Chen[23] proposed a dual-core PCF with a liquid-crystal core , and the ultrabroad bandwidth is also 250 nm. But the liquid crystal in Refs. [22] and [23] is easily affected by environment temperature. Hameed[24] proposed a polarization splitter with bandwidth of 75 nm, the soft glass PCF is filled with liquid crystal. Fan[25] designed a PCF polarization splitter filled with gold wire into the air holes, the bandwidth could reach to 47 nm in which the extinction ratio is lower than −12 dB. Sun[26] obtained a polarization splitter by using a PCF filled with Ag wire which has a bandwidth of 146 nm.

When metal is stimulated by light, the surface plasmon polaritons (SPPs) could be generated on the surface of the metal. The coupling characteristic between the two cores is affected by the metal wire or metal film filled or coated in the cladding air hole of PCF. The guided-core mode couples to the SPP mode when the phase matching condition is satisfied. Great progress has been made in the fabrication of filling and coating metal in PCF. In 2006, Sazio[27] reported the fabrication of high-quality Ge in PCF using the method of high-pressure microfluidic chemical deposition. In the experiment, a germanium tetrahydride GeH_4 flows past the PCF by the pressure of 2 MPa, simultaneously the PCF is heated. Amorphous germanium began to precipitate in the hole walls when the temperature exceeds 300 °C Celsius. Crystalline grains nucleate and grow as the temperature exceeds the crystallization point of ∼ 375 °C. In 2007, Zhang[28] coated silver film on hole wall selectively by the method of chemical deposition. In the progress, all the holes except one are blocked by glue at the end of the fiber preform. Then, the fiber end is connected to a syringe to allow suction of the reaction mixture of dextrose and silver nitrate. In 2008, Lee[29] filled gold into air holes selectively. First, they block all the holes of PCF except one hole by glue. Second, they heated the PCF to the softening point of glass which results that the blocked holes collapse and the open hole is enlarged by applying appropriate internal pressure. Then, molten gold is pumped into the enlarged hole by using the pressure of 190 bars (1 bar = 10^5 Pa). Therefore, it is possible to fabricate the proposed PCF with micron-scale gold wire with the development of science and technology.

In this paper, a broad-bandwidth polarization splitter based on soft glass-PCF filled with micron-scale gold wire is proposed. The bandwidth in which the extinction ratio is lower than −20 dB is 226 nm, i.e., from 1465 nm to 1691 nm which possesses great potential applications to adapt to the development of the high-speed and broadband communication system. The birefringence is increased and the coupling length is decreased by filling the gold wire into the air hole of PCF. The coupling length ratio is close to 2 under the optimized structural parameters. The resonance characteristics and the coupling length ratio are calculated and analyzed. The cure of coupling length ratio versus wavelength is flat which is useful to realize a broad-bandwidth polarization splitter. The polarization characteristics of tellurite glass-PCF and silica-PCF are also compared.

2. Geometry

The cross section of the proposed soft-tellurite-based PCF with micron-scale gold wire is shown in Fig. 1. Air holes are arranged in a hexagonal lattice, and lattice pitch is 2 μm. The two cores A, B are formed by removing two air holes. The diameter of air holes is d_1. Micron-scale gold wire is injected into the central hole of PCF, its diameter is d_2. The background material is tellurite glass of which the refractive index is determined by the sellmeier equation[30]

$$n_\lambda = \sqrt{A + \frac{B\lambda^2}{\lambda^2 - C} + \frac{D\lambda^2}{\lambda^2 - E}}, \tag{1}$$

where $A = 2.4843245$, $B = 1.6174321$, $C = 0.053715551$, $D = 2.4765135$, and $E = 225.0$. The refractive index of air is 1. The permittivity of gold is described by the Drude–Lorentz model[31]

$$\varepsilon_m = \varepsilon_\infty - \frac{\omega_D^2}{\omega(\omega - \mathrm{j}\gamma_D)} - \frac{\Delta\varepsilon \cdot \Omega_L^2}{(\omega^2 - \Omega_L^2) - \mathrm{j}\Gamma_L\omega}. \tag{2}$$

Gold will not have a chemical reaction with most chemicals and shows strong corrosion resistance. The ductility of Gold is the highest. Nowadays, the fabrication techniques for the preform of PCF include ultrasonic drilling, cast rod in tube, extrusion and stacking. We think the gold wire can be fabricated firstly. Then, filling the gold wire into the preform which can be drawn into the PCF. The finite element method[32] is used to investigate the characteristics of core mode and SPP mode. The computational region is meshed into 19650 elements for the structure $\Lambda = 2.0$ μm, $d_1 = 0.8$ μm, $d_2 = 0.8$ μm.

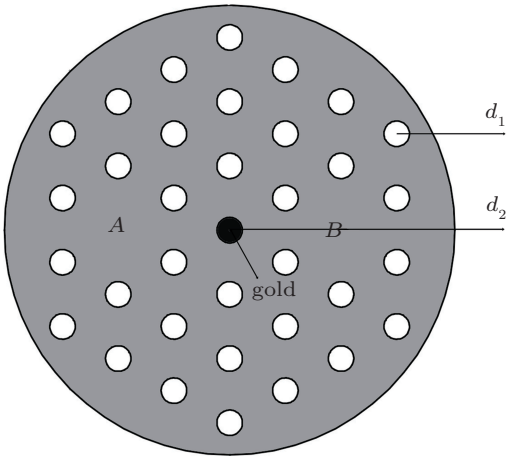


Fig. 1. Cross section of the proposed PCF with micron-scale gold wire. The background material is tellurite glass and the gold wire is injected into the central hole.

3. Results and discussion

According to the coupled-mode theory, there are four core guided modes which are even mode, odd mode of X-polarization and Y-polarization light shown in Figs. 2(a)–2(d).

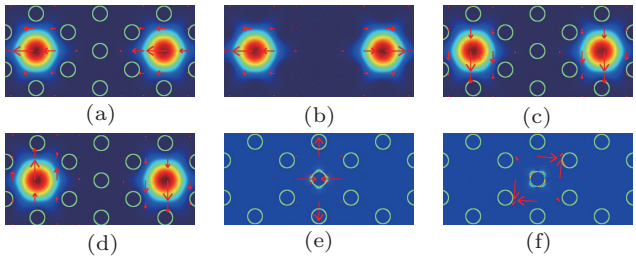


Fig. 2. (color online) The electric field distributions of (a) even mode, (b) odd mode of X-polarization light, (c) even mode, (d) odd mode of Y-polarization light, and (e) X-SPP mode, (f) Y-SPP mode.

The direction of arrow is the same for even mode, and it is the opposite for odd mode. The (e) X- and (f) Y-SPP modes are also shown in Fig. 2. The arrow represents the direction of electric field. When the phase matching condition is satisfied, core guided mode couples to SPP mode. In our considerable wavelength range, the odd mode of the X-polarization light couples to the X-SPP mode, and the odd mode of the Y-polarization light couples to the Y-SPP mode. The coupling characteristics of other order SPP modes and core guided modes are introduced in Ref. [33]. The loss of core guided mode is calculated by[32,34]

$$\alpha = 8.686 \times \frac{2\pi}{\lambda} \mathrm{Im}(n_{\mathrm{eff}}) \times 10^6, \tag{3}$$

where the unit of loss and wavelength are dB/m and μm respectively, $\mathrm{Im}(n_{\mathrm{eff}})$ represents the imaginary part of the effective refractive index of the mode. The effective refractive index and mode field distribution are calculated by the commercial software COMSOL Multiphysics based on the finite element method. The dispersion relation of core guided odd mode, SPP mode and loss spectra of core guided odd mode for (a) X-polarization and (b) Y-polarization light are shown in Fig. 3. Figure 3(a) shows the dispersion curves of X-polarization odd mode and X-SPP mode intersect at the wavelength 1.35 μm. The X-polarization odd mode couples to the X-SPP mode most strongly at the resonance wavelength and the loss could reach to 16125 dB/m. Figure 3(b) shows the dispersion curves of Y-polarization odd mode and Y-SPP mode intersect at the wavelength 1.353 μm. The Y-polarization odd mode couples to the Y-SPP mode most strongly at the resonance wavelength and the loss could reach to 7989 dB/m. The insets show the distribution of modal electric field at the resonance wavelength. The resonance loss of the X-polarization core mode is larger than that of the Y-polarization core mode, because that gold wire is in the X direction of the fiber core.

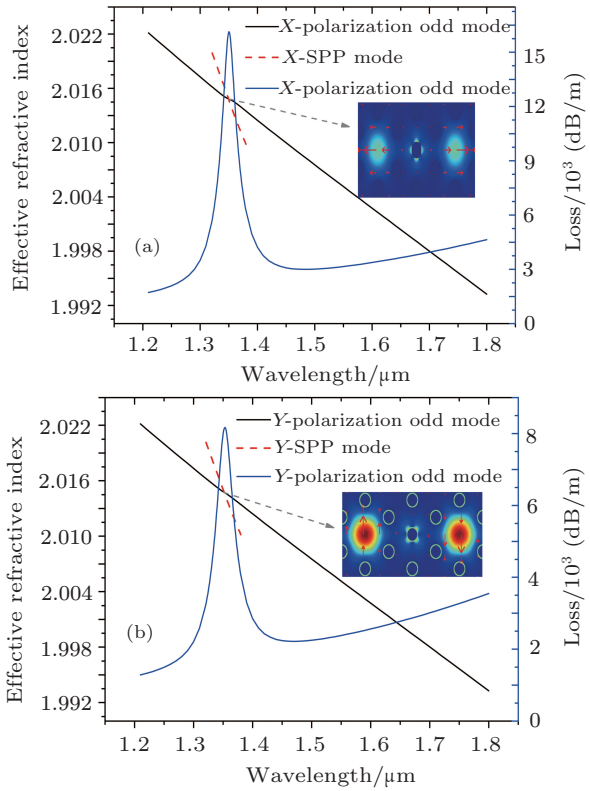


Fig. 3. (color online) Dispersion relation of core odd mode, SPP mode and loss spectra of core odd mode for (a) X-polarization and (b) Y-polarization light. The insets show the distribution of modal electric field at the resonance wavelength. The loss of X-polarization odd mode is larger than that of Y-polarization odd mode. The structural parameters used for the calculations are $d_1 = 0.8$ μm, $d_2 = 0.8$ μm, $\Lambda = 2.0$ μm.

Resonance wavelength should not be in the splitting wavelength range in order to obtain high output power of polarization splitter. Next, the characteristics of resonance loss are analyzed by adjusting the structural parameters of the PCF with micron-scale gold wire. Figure 4(a) shows the loss spectra of a core guided odd mode with different $d_1 = 0.6$, 0.8, 1.0 μm, and the other parameters are $d_2 = 0.8$ μm, $\Lambda =$ 2.0 μm. The odd mode happens to couple to the SPP mode, but the even mode does not couple to the SPP mode in the considerable wavelength range. So, we just need to analyze

the loss characteristics of the odd mode. The resonance wavelength the of odd mode red shifts slightly with increasing d_1. Because the refractive indices of odd mode and SPP mode decrease with increasing d_1, but that of the odd mode decreases much more, so the intersection of the dispersion curves of the odd mode and SPP mode red shifts slightly.

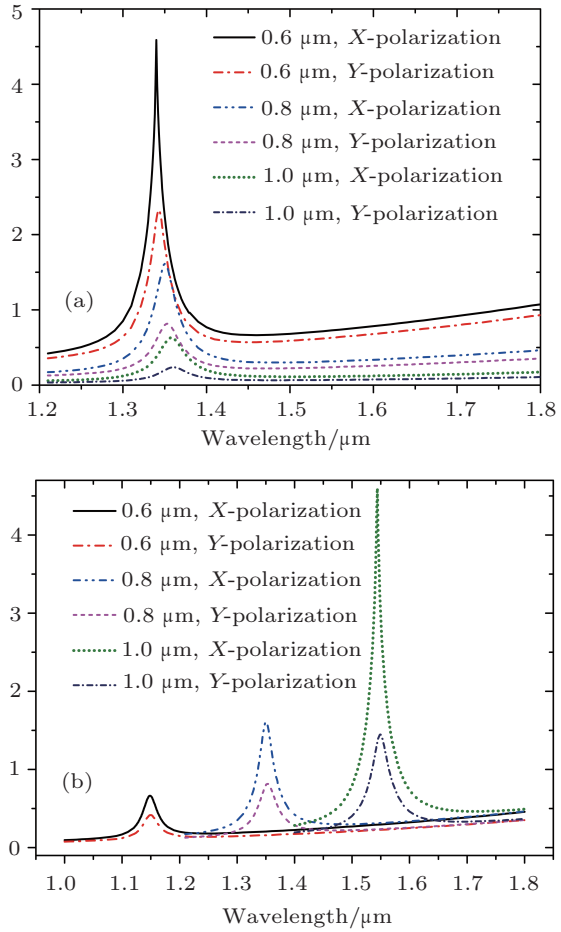


Fig. 4. (color online) Loss spectra for d_1 (a) 0.6, 0.8, 1.0 μm with the other parameters $d_2 = 0.8$ μm, $\Lambda = 2.0$ μm, and d_2 (b) 0.6, 0.8, 1.0 μm with the other parameters $d_1 = 0.8$ μm, $\Lambda = 2.0$ μm. The resonance wavelength red shifts and the resonance loss is decreased as increasing d_1 in panel (a), the resonance wavelength red shifts and the resonance loss is increased as increasing d_2 in panel (b).

The loss of the odd mode decreases with increasing d_1, because the odd mode is bound very tightly and the glass bridge between the fiber core and the gold wire becomes narrow, so the coupling between odd mode and SPP mode becomes difficult. Figure 4(b) shows the loss spectra of the core guided odd mode with different $d_2 = 0.6, 0.8, 1.0$ μm, and the other parameters are $d_1 = 0.8$ μm, $\Lambda = 2.0$ μm. It is similar to changing d_1 so that the odd mode just happens to couple to the SPP mode. The resonance wavelength of odd mode red shifts with the increase of d_2. Because the refractive index of the odd mode does not change nearly, but that of the SPP mode increases obviously, the result is the intersection of dispersion curves of odd mode and SPP mode red shifts.

The loss of odd mode increases with increasing d_2, because the distance between fiber core and gold wire becomes closer and much of the glass between two fiber cores is replaced by gold wire, so the coupling between odd mode and SPP mode becomes easier.

The polarization splitter of PCF is based on the interaction of even mode and odd mode which makes X-polarization or Y-polarization light coupling between core A and core B periodically. The coupling length, by which X-polarization or Y-polarization light couples from core A (B) to core B (A) completely, could be calculated by[35]

$$L_i = \frac{\lambda}{2|n_{\mathrm{i}}^{\mathrm{even}} - n_{\mathrm{i}}^{\mathrm{odd}}|}, \tag{4}$$

where n is the effective refractive index, λ represents the wavelength of incident light, and i expresses the x- or y polarization direction. The total fiber length is described by L. The incident light is input into one core. If L_x and L_y satisfy that $L = mL_x = nL_y$ where m and n are the positive integers with opposite parity, the X-polarization and Y-polarization light can be output in different fiber cores. In order to obtain a broadbandwidth polarization splitter, the next work is to get the coupling length ratio $m/n = 1:2$ or 2:1; by this way, L has strong tolerance in the wide wavelength range.

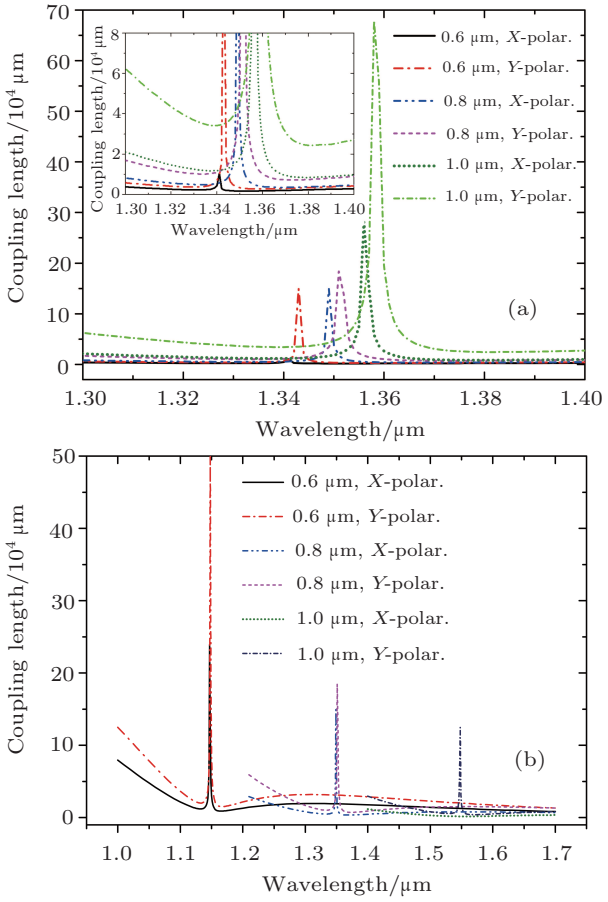


Fig. 5. (color online) Coupling length dependence on operable wavelength λ for d_1 (a) 0.6, 0.8, 1.0 μm with the other parameters $d_2 = 0.8$ μm, $\Lambda = 2.0$ μm, and d_2 (b) 0.6, 0.8, 1.0 μm with the other parameters $d_1 = 0.8$ μm, $\Lambda = 2.0$ μm. The coupling length has a peak due to the saltus of effective refractive index of odd mode at the resonance wavelength. The coupling length of X-polarization light does not have a peak when d_2 is 1.0 μm; we think it is because the calculation precision is not high enough.

Figure 5(a) shows the coupling length versus operable wavelength λ for d_1 0.6, 0.8, 1.0 μm, and the other parameters are $d_2 = 0.8$ μm, $\Lambda = 2.0$ μm. We could find that the coupling length of X-polarization or Y-polarization light has a peak value which is due to that the effective refractive index of odd mode has a saltus at resonance wavelength. The coupling length decreases with increasing d_1 due to the fact that the glass bridge decreases and the coupling of even mode and odd mode between the two cores becomes difficult. The coupling length of X-polarization light is 4789.6, 7935.9, and 17218.6 μm respectively at the communication wavelength of 1.55 μm, and that of Y-polarization light is 7044.3, 15242.6, and 48104.8 μm. Figure 5(b) reveals the coupling length versus the operable wavelength λ with different d_2 0.6, 0.8, 1.0 μm, and the other parameters are $d_1 = 0.8$ μm, $\Lambda = 2.0$ μm. We find the coupling length decreases rapidly at short wavelength before the resonance wavelength and becomes flat at the long wavelength range after the resonance wavelength. The flat coupling length is helpful to realize a broad-bandwidth polarization splitter. The coupling length of X-polarization light is 12588.4, 1935.9, 1548.8 μm at 1.55 μm, and that of Y-polarization light is 20058.0, 15242.6, 17596.5 μm.

Figure 6 shows the coupling length ratio (L_y/L_x) dependence on λ with different (a) d_1 under the other parameters $d_2 = 0.8$ μm, $\Lambda = 2.0$ μm, and with different (b) d_2 under the other parameters $d_1 = 0.8$ μm, $\Lambda = 2.0$ μm. The coupling length ratio increases with increasing d_1 or d_2 except for the resonance wavelength position of X-polarization or Y-polarization light. There is a peak at the resonance wavelength of Y-polarization and a trough at the resonance wavelength of X-polarization which can be understood by Fig. 5. But the coupling length ratio at the resonance wavelength is not changed regularly by varying d_1 or d_2, we guess this is due to the relatively low accuracy of the calculation. Numerical results show that $L_y = 15242.63$ μm, $L_x = 7935.94$ μm at the communication wavelength of 1.55 μm under the structural parameters $d_1 = 0.8$ μm, $d_2 = 0.8$ μm, $\Lambda = 2.0$ μm, and the coupling length ratio is 1.9207 close to 2. The resonance wavelength is not in our splitting wavelength range.

The light is assumed to be input into core A, normalized output power of X-polarization and Y-polarization light as transmittance distance in core A can be calculated by[36]

$$P_{i\text{-out}} = \cos^2\left(\frac{\pi \cdot L}{2 \cdot L_i}\right), \tag{5}$$

where L represents the fiber length or transmittance distance, L_i is obtained from Eq. (4).

Figure 7(a) reveals the variety of normalized power of 1.55 μm in core A as fiber length or propagation distance, the optimal structural parameters are $d_1 = 0.8$ μm, $d_2 = 0.8$ μm, $\Lambda = 2.0$ μm. As the fiber length or the propagation distance is 15871.88 μm, the X-polarization light is completely in core A, and, as the fiber length or the propagation distance is 15242.63 μm, the Y-polarization light is completely in core B. Extinction ratio (ER) is a vital parameter to evaluate the performance of the polarization splitter, the incident light is assumed to be input into core A, then the extinction ratio in core A could be obtained by[15]

$$\mathrm{ER} = 10 * \lg\left(\frac{P_{y\text{-out}}}{P_{x\text{-out}}}\right). \tag{6}$$

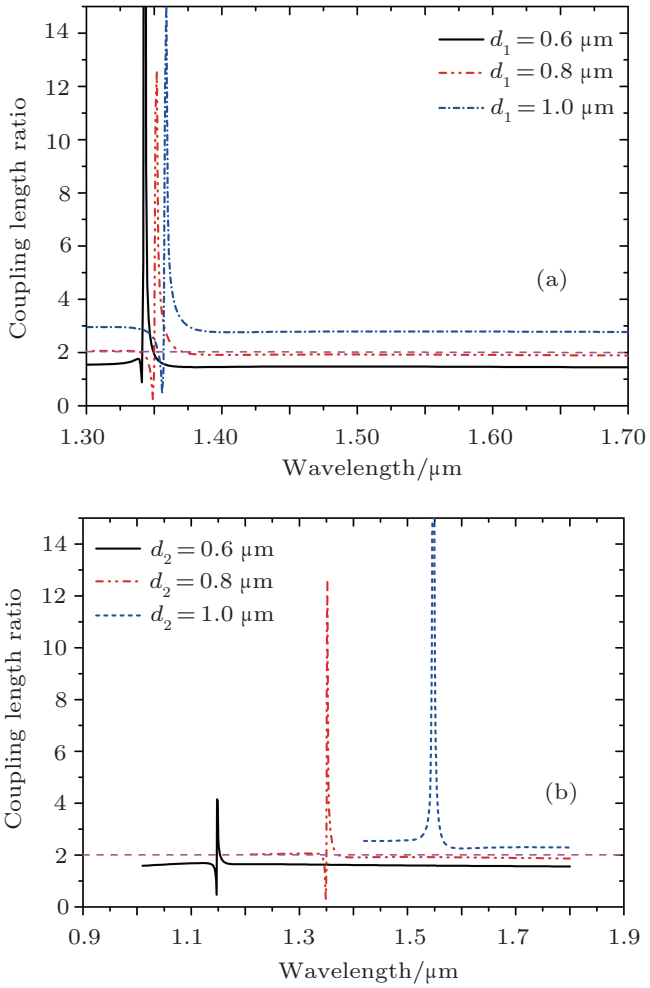


Fig. 6. (color online) Coupling length ratio versus the operable wavelength λ with different (a) d_1 under the other parameters $d_2 = 0.8$ μm, $\Lambda = 2.0$ μm, and with different (b) d_2 under the other parameters $d_1 = 0.8$ μm, $\Lambda = 2.0$ μm. The coupling length ratio has a peak at the resonance wavelength of Y-polarization light and has a trough at the resonance wavelength of X-polarization light.

When the extinction ratio is larger (lower) than 20 (-20) dB, the vertical polarized lights could be separated very well. Figure 7(b) reveals that the extinction ratio versus the op-

erable wavelength λ with different fiber lengths under the optimal structural parameters, the fiber length is 13900, 14100, 14300, 14500, 14700 μm respectively. We could find that ER at the communication wavelength of 1.55 μm decreases with increasing fiber length, but the bandwidth in which ER is lower than −20 dB becomes narrow. As the fiber length is 14300 μm, extinction ratio in the wavelength range 1465 nm–1691 nm is lower than −20 dB, the corresponding bandwidth could reach to 226 nm.

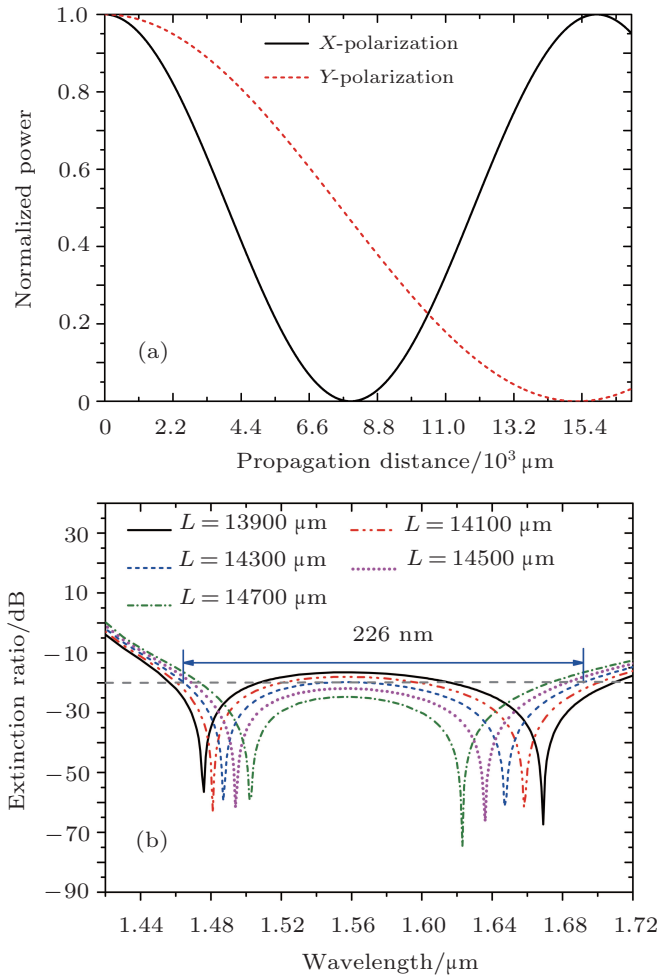


Fig. 7. (color online) (a) Normalized power of 1.55 μm versus the propagation distance, the coupling length of X-polarization, Y-polarization light is 7935.94 μm and 15242.63 μm, and (b) the extinction ratio versus the operable wavelength λ with different fiber length under the optimal structural parameters, the bandwidth in which the extinction ratio is lower than −20 dB is 226 nm as the fiber length is 14300 μm.

The insertion loss (IL) is also a key factor to measure the polarization beam splitter, which could be calculated by the following equation[37]

$$\mathrm{IL} = -10 * \lg\left(\frac{P_{x\text{-out}}}{P_{x\text{-in}}}\right). \tag{7}$$

Figure 8 reveals the insertion loss versus the operable wavelength λ under the optimized structural parameters $d_1 = d_2 = 0.8$ μm, $\Lambda = 2.0$ μm. There is a peak of the curve in the wavelength range 1.45 μm–1.70 μm, the insertion loss at the wavelength of 1.55 μm is not the minimal, because the fiber length is not the best optimized for 1.55 μm to realize a broadband polarization splitter. The insertion loss is 0.00248 dB, 0.42737 dB, and 0.00114 dB at the wavelength of 1.47 μm, 1.55 μm, and 1.69 μm respectively. The insertion loss is lower than 0.44 dB in our considerable wavelength range 1.465 μm–1.691 μm. In the long wavelength, the insertion loss increases as the wavelength increases.

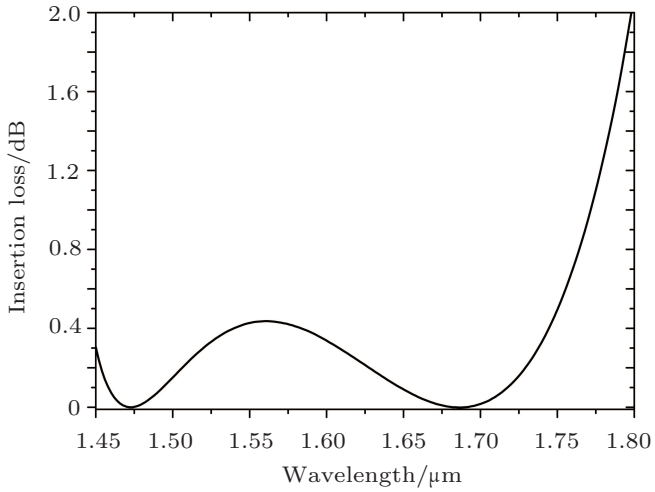


Fig. 8. Insertion loss versus the operable wavelength λ under the optimized structural parameters. There is a peak in our considerable wavelength range. The insertion loss is just 0.00248 dB and 0.42737 dB at the wavelength of 1.47 μm, 1.55 μm. The insertion loss increases as wavelength increases in the long wavelength.

The fabrication tolerance of the designed polarization splitter is also analyzed, as shown in Fig. 9. The structural parameters fluctuate up and down two percent. The bandwidth in which the extinction ratio is lower than −13 dB is 210 nm, i.e., from 1470 nm to 1680 nm as d_1 is changed to $d_1 \times 0.98$ as shown in Fig. 9(a). The curve just has one peak which we think is related to the optical fiber length. The extinction ratio at the wavelength of 1.55 μm is −34 dB, and the corresponding bandwidth is 330 nm, i.e., from 1440 nm to 1770 nm as d_1 is $d_1 \times 1.02$ as shown in Fig. 9(a). The bandwidth in which the extinction ratio is lower than −13 dB is 310 nm, i.e., from 1420 nm to 1730 nm as d_2 is changed to $d_2 \times 0.98$ as shown in Fig. 9(b), and the bandwidth is 240 nm, i.e., from 1480 nm to 1720 nm as d_2 is $d_2 \times 1.02$, the extinction ratio at the wavelength of 1.55 μm is −37 dB. The minimal extinction ratio in our considerable wavelength range is −61 dB at the wavelength of 1.62 μm. Lastly, d_1, d_2 are simultaneously changed. As d_1, d_2 are changed to d_1, $d_2 \times 0.98$, the bandwidth in which the extinction ratio is lower than −13 dB is 250 nm, i.e., from 1440 nm to 1690 nm as shown in Fig. 9(c), and the corresponding bandwidth is 310 nm, i.e., from 1460 nm to 1770 nm as d_1, d_2 are d_1, $d_2 \times 1.02$.

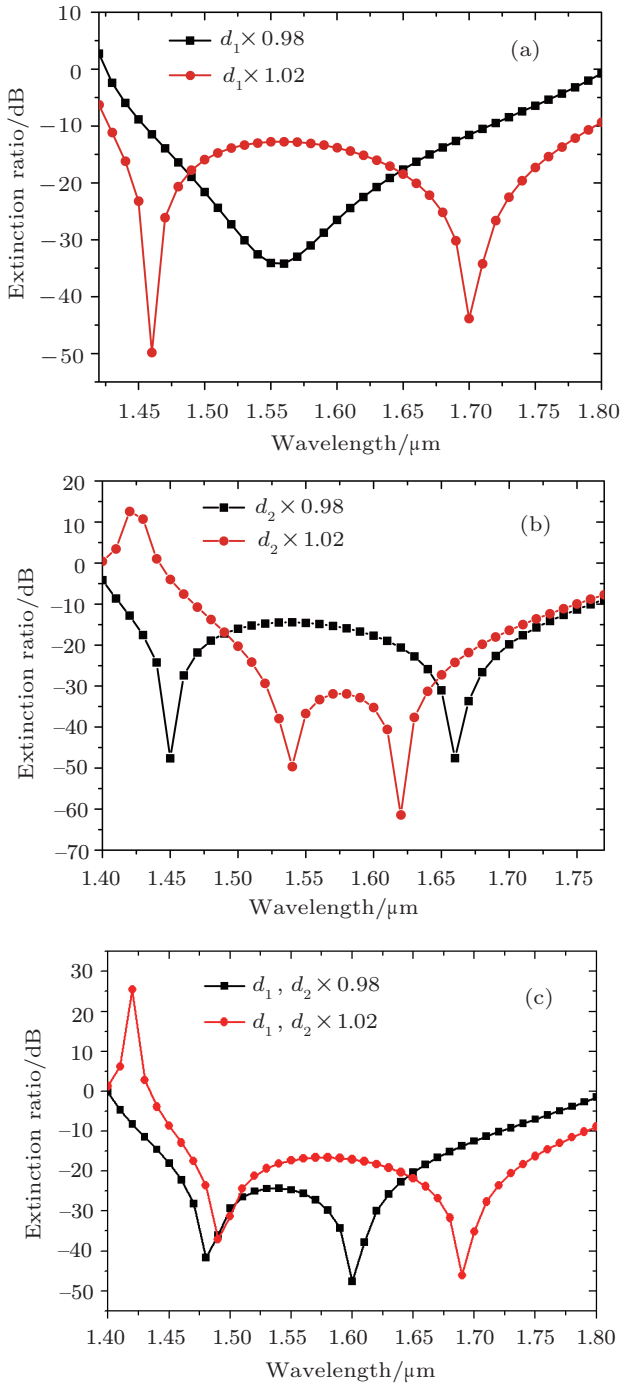


Fig. 9. (color online) The fabrication tolerance of the designed polarization splitter is considered, the structural parameters fluctuate up and down two percent. d_1 is changed to $d_1\times 0.98$ and $d_1\times 1.02$, the bandwidth in which the extinction ratio is lower than -13 dB is 210 nm, 330 nm respectively in panel (a), d_2 is changed to $d_2\times 0.98$ and $d_2\times 1.02$, the bandwidth in which the extinction ratio is lower than -13 dB is 310 nm, 240 nm in panel (b), d_1, d_2 are changed to $d_1\times 0.98$ and $d_1\times 1.02$, the bandwidth in which the extinction ratio is lower than -13 dB is 250 nm, 310 nm in panel (c).

The coupling length and coupling length ratio based on the PCF without gold wire are shown in Fig. 10. The solid line represents the X-polarization light, and the dash line is the Y-polarization light. The coupling length decreases as wavelength increases. Compared with Fig. 7, we see the coupling length could be greatly reduced by introducing gold wire into the PCF. The coupling length of X-polarization, Y-polarization light is 31220 μm, 39727 μm at the wavelength of 1.55 μm. The large coupling length is not convenient to fabricate a tiny polarization splitter. The coupling length ratio is far less than 2, and it is just 1.27 at the wavelength 1.55 μm.

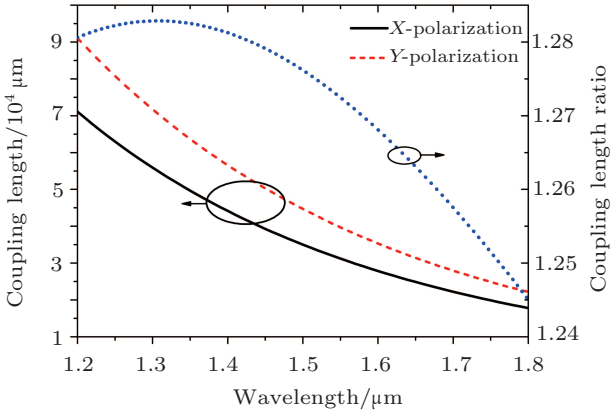


Fig. 10. (color online) Coupling length and coupling length ratio versus the operable wavelength λ based on the tellurite glass-PCF without gold wire, the structural parameters are $d_1 = 0.8$ μm, $d_2 = 0.8$ μm, and $\Lambda = 2.0$ μm.

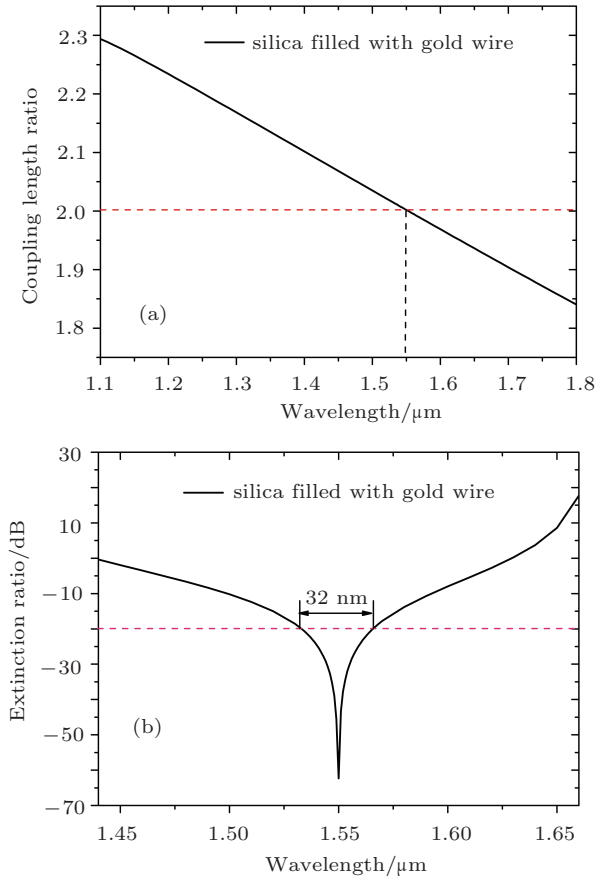


Fig. 11. (color online) (a) Coupling length ratio and (b) extinction ratio versus the operable wavelength λ based on silica-based PCF filled with Gold wire, the optimized structural parameters are $d_1 = 1.034$ μm, $d_2 = 0.8$ μm, and $\Lambda = 2.0$ μm.

Figure 11 illustrates the variation of (a) coupling length ratio and (b) extinction ratio with operable wavelength λ based on silica-based PCF filled with gold wire, the structural parameters are $d_1 = 1.034$ μm, $d_2 = 0.8$ $u\mu$m, and $\Lambda = 2.0$ μm, and the fiber length is 8100 μm. The horizontal dash line repre-

sents that the coupling length ratio is 2, the vertical line indicates the wavelength 1.55 μm in panel (a). Coupling length ratio is 2 at 1.55 μm, but the curve of the variety of coupling length ratio with wavelength is not flat which is not helpful to obtain a broad-bandwidth polarization splitter. ER could reach to −62.3 dB at 1.55 μm, and the bandwidth of ER lower than −20 dB is just 32 nm. The horizontal dash line represents that the extinction ratio is −20 dB. The bandwidth based on tellurite glass is further better than that based on silica glass.

We also calculate the birefringence B based on the silica-based and tellurite-based PCF with or without metal wire. Figure 12 shows the birefringence B versus the operable wavelength λ, the structural parameters are $d_1 = 0.8$ μm, $d_2 = 0.8$ μm, and $\Lambda = 2.0$ μm. The birefringence B based on silica-based PCF with gold wire is much higher than that based on tellurite-based PCF with gold wire, the birefringence B are 23.7×10^{-5} and 3.8×10^{-5} at the wavelength of 1.55 μm respectively. So the coupling length based on silica-based PCF is much shorter than that based on tellurite-based PCF. The birefringence B based on silica-based PCF without gold wire is also higher than that based on tellurite-based PCF without gold wire, and the birefringence B are 2.5×10^{-5} and 1.0×10^{-5} at the wavelength of 1.55 μm. We also could see that the birefringence B of PCF with gold wire is much higher that that of PCF without gold wire. It further proves that the coupling length could be decreased by introducing gold wire.

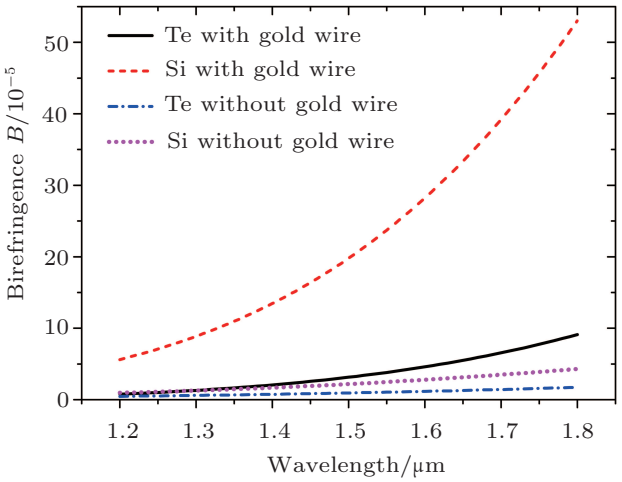


Fig. 12. (color online) The birefringence B versus the operable wavelength λ based on tellurite-based and silica-based PCF with or without gold wire, the structural parameters are $d_1 = 0.8$ μm, $d_2 = 0.8$ μm, and $\Lambda = 2.0$ μm. The birefringence B is improved by introducing gold wire into PCF.

4. Conclusion

To summarize, a broad-bandwidth polarization splitter based on soft glass photonic crystal fiber filled with gold wire in the central hole is proposed. The coupling characteristics and resonance characteristics are analyzed by adjusting structural parameters using the finite element method. The coupling length ratio is 1.9207 at the communication wavelength of 1.55 μm and the variation curve of coupling length ratio with wavelength is flat in the splitting wavelength range under the optimal structural parameters $d_1 = 0.8$ μm, $d_2 = 0.8$ μm, and $\Lambda = 2.0$ μm. The bandwidth in which the extinction ratio is lower than −20 dB is 226 nm. The broad-bandwidth polarization splitter will be widely used with the development of a high-speed and broadband communication system. By comparison, we find the bandwidth based on tellurite glass is further better than that based on silica glass. We also demonstrate that the birefringence could be improved by introducing gold wire into PCF. The polarization splitter shows broad bandwidth, low insertion loss, simple structure and high fabrication tolerance.

References

[1] Taillaert D, Chong H, Borel P I, Frandsen L H, Rue R M D L and Baets R 2003 *IEEE Photon. Technol. Lett.* **15** 1249
[2] Dai D 2012 *J. Lightwave Technol.* **30** 3281
[3] Tang Y, Dai D and He S 2009 *IEEE Photon. Technol. Lett.* **21** 242
[4] Yamazaki T, Aono H, Yamauchi J and Nakano H 2008 *J. Lightwave Technol.* **26** 3528
[5] Guan X, Wu H, Shi Y, Wosinski L and Dai D 2013 *Opt. Lett.* **38** 3005
[6] Peng G, Tjugiarto T and Chu P 1990 *Electron. Lett.* **26** 682
[7] Russell P St J 2006 *J. Lightwave Technol.* **24** 4729
[8] Song Y, Hu M, Wang C, Tian Z, Xing Q, Chai L and Wang C 2008 *IEEE Photon. Technol. Lett.* **20** 1088
[9] Cucinotta A, Poli F and Selleri S 2004 *IEEE Photon. Technol. Lett.* **16** 2027
[10] Zhu X P, Li S, Du Y, Han Y, Zhang W, Ruan Y, Heike E, Shahraam A and Tanya M M 2013 *Chin. Phys. B* **22** 014215
[11] Matsui T, Nakajima K and Sankawa I 2007 *J. Lightwave Technol.* **25** 757
[12] Chen L, Zhang W, Wang L, Bai Z, Zhang S, Wang B, Yan T and Jonathan S 2014 *Chin. Phys. B* **23** 104220
[13] Qin W, Li S, Xue J, Xin X and Zhang L 2013 *Chin. Phys. B* **22** 074213
[14] Zhang L and Yang C 2004 *IEEE Photon. Technol. Lett.* **16** 1670
[15] Saitoh K, Sato Y and Koshiba M 2004 *Opt. Express* **12** 3940
[16] Chiang J, Sun N, Lin S and Liu W 2010 *J. Lightwave Technol.* **28** 707
[17] Chen M, Sun B, Zhang Y and Fu X 2010 *Appl. Opt.* **49** 3042
[18] Zhang L and Yang C 2003 *Opt. Express* **11** 1015
[19] Liu S, Li S, Yin G, Feng R and Wang X 2012 *Opt. Commun.* **285** 1097
[20] Zhang L and Yang C 2004 *J. Lightwave Technol.* **22** 1367
[21] Jiang H, Wang E, Zhang J, Hu L, Mao Q, Li Q and Xie K 2014 *Opt. Express* **22** 30461
[22] Hameed M F O and Obayya S S A 2011 *IEEE J. Quantum Electron.* **47** 1283
[23] Chen H, Li S, Fan Z, An G, Li J and Han Y 2014 *IEEE Photon. J.* **6** 1
[24] Hameed M F O and Obayya S S A 2009 *IEEE Photon. J.* **1** 265
[25] Fan Z, Li S, Fan Y, Zhang W, An G and Bao Y 2014 *Chin. Phys. B* **23** 094212
[26] Sun B, Chen M, Zhou J and Zhang Y 2013 *Plasmonics* **8** 1253
[27] Sazio P J A, Amezcua C A, Finlayson C E, *et al.* 2006 *Science* **311** 1583
[28] Zhang X, Wang R, Cox F M, Kuhlmey B T and Large M C J 2007 *Opt. Express* **15** 16270
[29] Lee H W, Schmidt M A, Tyagi H K, Sempere L P and Russell P St J 2008 *Appl. Phys. Lett.* **93** 111102
[30] Ghosh G 1995 *J. Am. Ceram. Soc.* **78** 2828
[31] Vial A, Grimault A, Macías D, Barchiesi D and Chapelle M 2005 *Phys. Rev. B* **71** 085416
[32] Liu Q, Li S and Chen H 2015 *IEEE Photon. J.* **7** 2700210
[33] Nagasaki A, Saitoh K and Koshiba M 2011 *Opt. Express* **19** 3799
[34] Kuhlmey B, Renversez G and Maystre D 2003 *Appl. Opt.* **42** 634
[35] Zhang S, Yu X, Zhang Y, Shum P, Zhang Y, Xia L and Liu D 2012 *IEEE Photon. J.* **4** 1178
[36] Florous N, Saitoh K and Koshiba M 2005 *Opt. Express* **13** 7365
[37] Chang K and Huang C 2016 *Sci. Rep.* **6** 19609